Journal of Research and Applications in Mechanical Engineering
ISSN: 2229-2152 (Print); 2697-424x (Online)
(2025) Vol. 13, No. 1, Paper No. JRAME-25-13-006
[DOI: 10.14456/jrame.2025.6]

Research Article

Transient Heat Transfer in 2D Air Jet Impingement on High-Temperature Plate

Y.S. Bisht[1]
S.D. Pandey[1]
S. Chamoli[2,*]
[1] *Department of Mechanical Engineering, Uttaranchal Institute of Technology, Uttaranchal University, 248007, India*
[2] *Department of Mechanical Engineering, Govind Ballabh Pant Institute of Engineering & Technology, India*

Received 5 January 2024
Revised 15 April 2024
Accepted 27 April 2024

Abstract:
This study explores the transient heat transfer characteristics of two-dimensional air-jet impingement on a heated surface. Utilizing numerical methods, the research comprehensively analyzes thermal behavior and transient heat transfer mechanisms, considering varied jet parameters, plate temperatures, and time. The investigation covers Reynolds numbers (Re) in the range of 3000 to 12000, based on the hydraulic diameter, with nozzle diameters (Dj) of 3mm, 4mm, and 5mm. The nozzle jet-to-plate distance (H/D) is varied from 0.2 to 2. Results reveal substantial variations in Nusselt numbers (Nu) corresponding to changes in Re and jet-to-plate distance. In addition, approximately Re 12000 the largest friction factor occur at 3mm jet diameter. The Notably, heat transfer near the stagnation point intensifies with decreased jet-to-plate distance, while heat transfer near the boundary point diminishes. These findings offer valuable insights for practical applications in thermal management and heat exchanger design.

Keywords: *Transient analysis, Jet impingement, Heat transfer, CFD, Thermo-hydraulic performance*

1. Introduction

In various industrial applications such as metal processing, electronics cooling, and aerospace propulsion, the impingement of high-velocity air jets onto heated surfaces plays a crucial role in thermal management and energy transfer processes. Understanding transient heat transfer phenomena in such configurations is paramount for optimizing system efficiency, ensuring product quality, and mitigating thermal stresses. In this paper, we focus on investigating the transient heat transfer characteristics of a two-dimensional (2D) air jet impinging on a high-temperature plate. Numerous studies have explored the heat transfer enhancement potential and flow characteristics associated with jet impingement techniques. Bisht et al. [1] conducted a comprehensive review outlining future research trends in jet impingement heat transfer enhancement. Sheikholeslami et al. [2] provided insights into recent advancements in flat plate solar collectors and photovoltaic systems in the presence of nanofluids, shedding light on heat transfer augmentation techniques. Pukhovoy et al. [3] investigated extreme heat fluxes and heat transfer mechanisms during electronics cooling using spray and jet impingement methods, emphasizing the importance of understanding transient phenomena. Diop et al. [4] studied heat transfer characteristics by impinging jet with various velocity distributions, offering valuable insights into flow regimes and their impact on heat transfer performance. Jiang et al. [5] explored the influence of geometric modifications on fuel mixing and combustion in supersonic

* Corresponding author: S. Chamoli
E-mail address: mech.chamoli@gmail.com

combustion chambers, demonstrating the relevance of jet flow control in enhancing performance. Farnham et al. [6] evaluated the cooling effects of outdoor water mist fans, highlighting practical applications of impinging jet technology in environmental control.

Experimental investigations by Bisht et al. [7] analyzed jet impingement heat transfer in a channel flow embedded with V-shaped patterned surfaces, providing experimental data for validation of numerical models. Jiang et al. [8] investigated the effect of upstream angled ramps on fuel mixing of hydrogen jets at supersonic crossflows, contributing to the understanding of flow control mechanisms. Sheikholeslami and Farshad [9] conducted numerical simulations to study the effect of non-uniform solar irradiation on nanofluid turbulent flow, emphasizing the importance of considering environmental factors in heat transfer analyses. Furthermore, studies by Yaga et al. [10] and Jiang et al. [11] explored the effect of surface modifications on mixing performance and heat transfer behavior in supersonic flow regimes, providing valuable insights into flow-surface interactions. Nuntadusit et al. [12] investigated heat transfer enhancement on the surface of an impinging jet by increasing entrainment using air-augmented ducts, proposing practical solutions for heat transfer augmentation. The relationship for single slot impinging jets was found to depend on geometric parameters such as Reynolds number, jet-to-surface spacing, and jet width. The concept of jet impingement for steam-assisted heating (SAH) was initially introduced [13]. This study investigated the geometric parameters of SAHJI including hole diameter, interspacing, and height between the heated surface and jet plate, under various mass flow rates and channel lengths. The results demonstrated that SAHJI exhibited superior heat transfer capabilities compared to SSAH.

Analyzing the thermal efficiency of an unglazed solar air heater with a jet plate, it was determined, that jet spacing was a significant factor affecting performance. A study delved into the thermal characteristics of SAH systems utilizing staggered and inline jet arrays. The research indicated that Computational Fluid Dynamics (CFD) simulations could effectively evaluate factors such as jet-to-plate spacing, as well as impinging patterns, local Nusselt number dispersal, and pressure drop. SAH was designed [14] to modify the design of a slot jet and explore the impact of Re and nozzle-to-heated-plate spacing. Investigating flow and geometric parameters for SAHJI revealed a heat transfer enhancement of 2.66 to 3.50 times, accompanied by an increase in friction factor within the duct. Sheikholeslami et al. [15] conducted a study examining the flow and geometric parameters of SAHJI, uncovering a maximum heat transfer enhancement of 2.66 to 3.50 times, albeit with a corresponding increase in friction factor within the duct. Employing the Taguchi method, the contribution ratios of jet diameter, spanwise pitch ratio, and streamwise pitch ratio toward overall efficiency were determined as 48.86%, 41.61%, and 9.53%, respectively [16, 17]. In a different study, the exergetic and energy approach were identified as optimal for single-pass double duct jet plate operations. The study determined optimal values for X/D, Y/D, and Dj/D as 1.739, 0.869, and 0.0650, respectively, achieving a maximum exergetic efficiency of 4.36% [18]. An experimental approach was also employed to enhance thermohydraulic performance and increase heat transfer [19, 20] analyzed the performance of a single nozzle jet when adjusted for different nozzle diameters and angles of attack. The study revealed that employing different jet configurations on a rough surface can enhance the heat transfer process. Various parameters were examined in the study, and it was determined that the optimal heat transfer configuration involved jets set at specific height and diameter ratios corresponding to the chosen parameters. Research related to (SAH) with impinging jets has primarily relied on experimental methods, although some recent investigations have utilized computational techniques. As previously mentioned in the presentation of published works, several researchers have explored the effects of a roughened absorber plate and jet impingement on the efficiency of SAH.

The research gap of the current article is

- Quantify the impact of transient heat transfer phenomena on cooling efficiency.
- Explore the influence of different high-temperature plate materials on heat transfer characteristics.
- Optimize cooling strategies for high-temperature applications using 2D air jet impingement.
- Validate numerical models with experimental data to improve accuracy.
- Investigate innovative techniques to enhance heat transfer rates.
- Study multi-physics interactions between heat transfer and other phenomena

In contrast, the impact of discrete crossflow on induced air movement through a perforated jet plate within SAH has revealed previously uninvestigated effects. No studies have been conducted concerning SAH in which airflow originates from the lower chamber and travels all the way to the upper chamber via the perforated jet plate using transient numerical simulations, resulting in heat transfer to the moving air due to crossflow. Consequently, an

endeavor has been undertaken to examine the effectiveness of SAH when there is crossflow-induced movement of air within the absorber portion featuring perforations in the Jet plate. This, in turn, leads to an enhancement in the thermo-hydraulic performance of SAH.

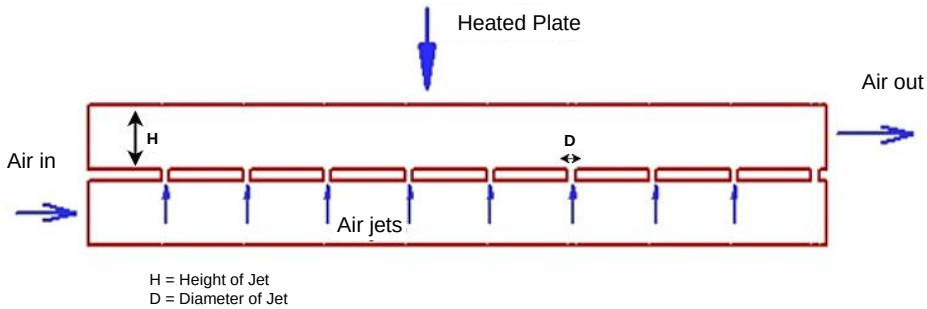

Fig. 1. Schematic diagram of jet impingement 2D Model.

2. Computational Domain

The 2D model for SAH which is rectangular in shape consisting of Jet plate of 1m length is depicted in Fig. 1. The jet plate is designed to have holes/slots with diameter Dj. The jet diameters of 3mm, 4mm and 5mm is considered in the present investigation named with Case 1, Case 2 and Case 3, respectively. The top portion of the channel is administered with constant heat flux of 1000 w/m2. The cases considered for the analysis in the present research work is depicted in Table 1.

Table 1: Cases studied in the present numerical simulation.

Case	Jet Diameter (D_j) mm	Jet Height (H) mm	H/D Ratio
Case I	3 mm	0.6 mm	0.2
Case II	4 mm	4.4 mm	1.1
Case III	5 mm	10 mm	2

2.1. Numerical Methodology

In this work, a two-dimensional jet discharging from a slot nozzle impinging normally onto a solid plate heated by a uniform source as shown in Fig. 1 investigated. The fluid considered is incompressible, the equations for conservation of mass, momentum, and energy in the Cartesian coordinate are represented in equations 1 to 3.
Continuity Equation

$$\nabla \cdot \left(\rho_f \vec{V}\right) = 0 \tag{1}$$

Momentum Equation

$$\vec{V} \cdot \nabla\left(\rho_f \vec{V}\right) = -\nabla P + \nabla.\left(\mu_f \nabla \vec{V}\right) \tag{2}$$

Energy Equation for Fluid

$$\vec{V}.\nabla\left(\rho_f C_{pf} T_f\right) = \nabla.\left(k_f \nabla T_f\right) \tag{3}$$

The objective of present 2D simulations is to conduct a time-based study on transient flow patterns. In the current study, we focused on assessing the impact of jet diameter on heat transfer enhancement under transient conditions. In addition, the present work focused on a 2D jet impingement heat transfer simulation is to gain insight into the fundamental flow and heat transfer mechanisms involved in fluid jet impingement on a target surface. Central to this objective is the analysis and understanding of heat transmission by the impinging jet, which includes studying the distribution of heat transfer coefficients on the target surface and the effects of jet parameters on heat transfer,

including the occurrence of hotspots. The time step for the present study is taken as 0.1s. The expected flow structure in the jet impingement based on the literature survey is depicted in Fig. 2.

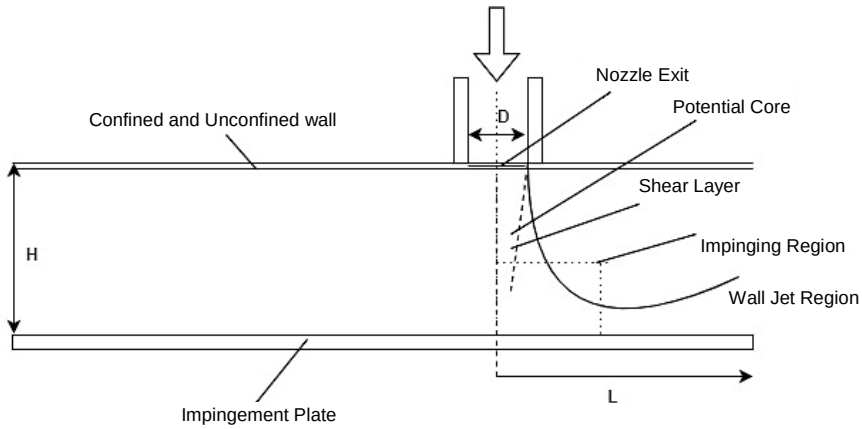

Fig. 2. The theorized flow pattern in the jet impingement hat transfer model.

2.2. Grid independency

To attain grid independence, the mesh domain of the baseline model employs a range of 0.4 to 2 million elements. No significant changes are observed as the grid is expanded from 2 million to 3 million elements. The determination of grid-independent criteria based on a comparison of Nu. Fig. 3 represents the meshing used in the present computational domain. In both the baseline model (with components ranging from 0.4 to 2 million) and the perforated model (with components ranging from 1.0 to 3 million), the difference in Nu is less than 2%, as depicted in Fig. 3. Consequently, an analysis is conducted using 2.8 million components for the baseline configuration and approximately 3 million elements for the jet plate configuration to optimize processing time.

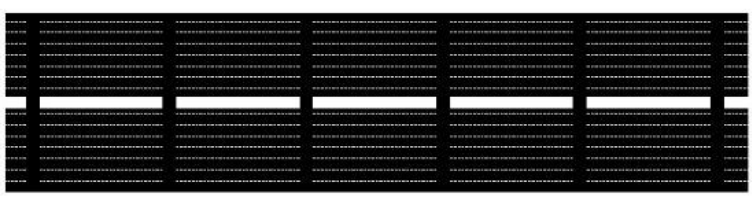

Mesh domain of the basic model uses 0.4 million to 2 million elements no change in Nu

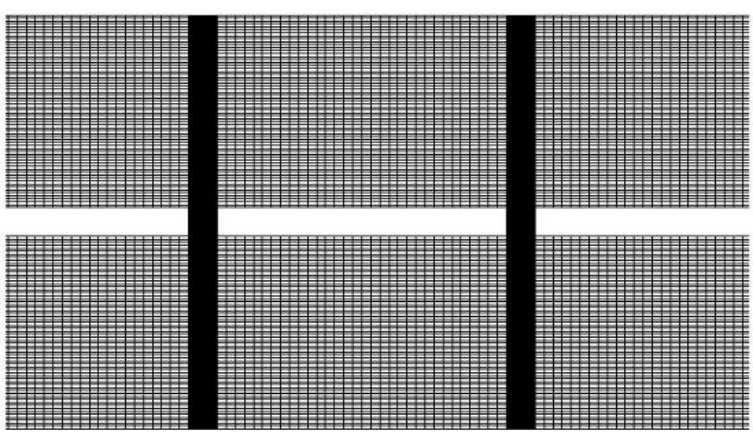

Mesh domain of the basic model uses 2 million to 3 million elements 2% change in Nu

Fig. 3. Grid independency with different grid and their effect on Nu

3. Results and Discussion

3.1 Effect of jet diameter on 2D simulation jet impingement heat transfer

In a 2D simulation of jet impingement, the diameter of the impinging jet can significantly affect the heat transfer properties. In this article, the jet diameter to jet impingement height ratio ($D/H \geq 0.33$) leads to several major effects: Size of the Impingement Zone: The size of the impingement zone on the target surface is contingent upon the diameter of the jet. A larger jet diameter covers a greater surface area within the impingement zone. This expanded coverage can result in more uniform cooling or heating, along with a wider distribution of heat transmission.

Flow Structure: The jet diameter influences the flow pattern in the vicinity of the impingement area. A larger jet diameter leads to a broader dispersion of the jet flow, creating a larger and more diffused impingement footprint. Consequently, a wider and more scattered region of intense heat transfer may emerge. This could have implications for regional heat transfer coefficients and temperature gradients.

Jet Development Length: The jet diameter impacts the length of the jet's flow before impingement. For a larger jet diameter, the flow needs to traverse a greater distance to attain a fully developed velocity profile upon impingement. This can influence the characteristics of heat transfer, affecting velocity and temperature profiles at the impingement surface.

Impingement Heat Transfer Coefficient: The impingement heat transfer coefficient is directly affected by the jet diameter. A larger jet diameter results in increased impingement area, velocity, and thermal mixing. Consequently, the average heat transfer coefficient is often higher. However, variations might exist in the distribution of heat transfer coefficients across the impingement surface, with regions closer to the jet's centerline potentially exhibiting faster heat transfer rates.

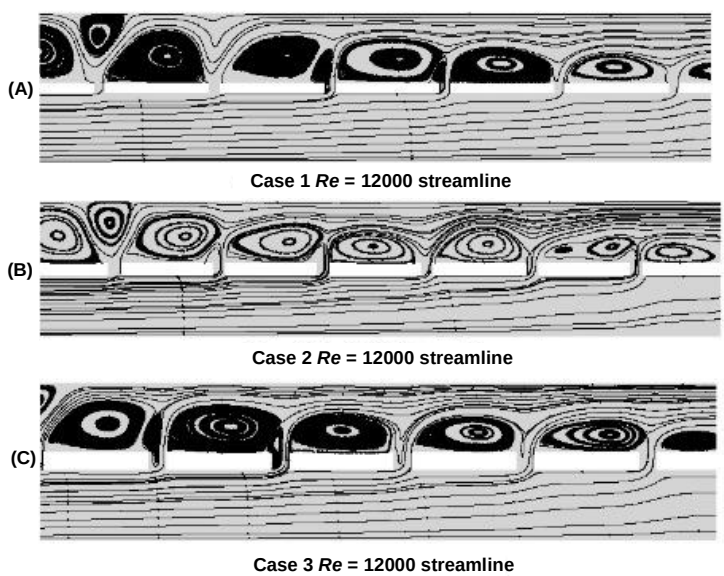

Fig. 4. Flow streamlined projection along the mid-x-y axis for Re = 12000 for a) Case 1, b) Case 2, and c) Case 3.

The flow and heat transfer behavior of impinging square jets were elucidated by [20] through the projection of flow lines. In situations where H/D exceeded 0.27, observable were the periphery vortices of the jet and the upwash flow close to the point of jet collision. At H/D = 0.27, as the wall jets covered the full plate-to-plate distance, no upwash fountain was formed. Fig. 4 depicted stream flow lines and two rotating flow vortices observed for Jet diameter of 4 mm and thus this contributes better fluid flow mixing and better convective heat transfer rate and thus maximum Nu is obtained at jet diameter of 3 mm. These streamlines results are consistent with the vorticity results represented in Fig. 5. For better understanding of fluid flow structure, the velocity vector is represented for the three studied cases and presented in Fig. 6. The vectors originating from the jets impinges on the heated plate clearly replicated in

Fig. 5. The maximum vorticity is obtained at the jet diameter of 3 mm i.e. Case 1 in Fig. 6 and thus this results of better fluid flow mixing and thus maximum Nu is attained.

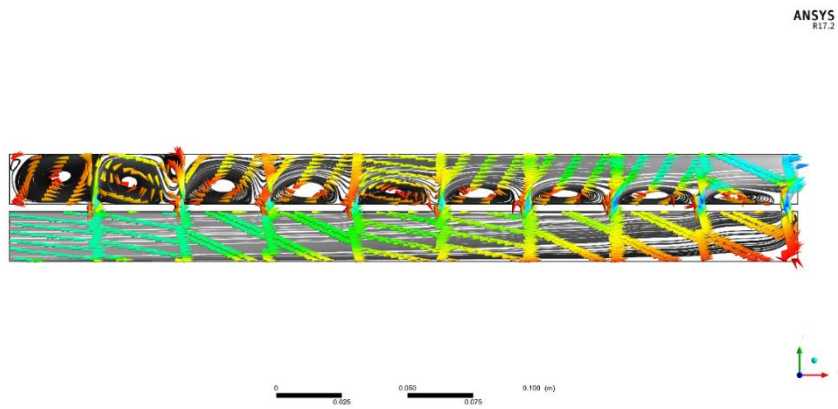

(a)

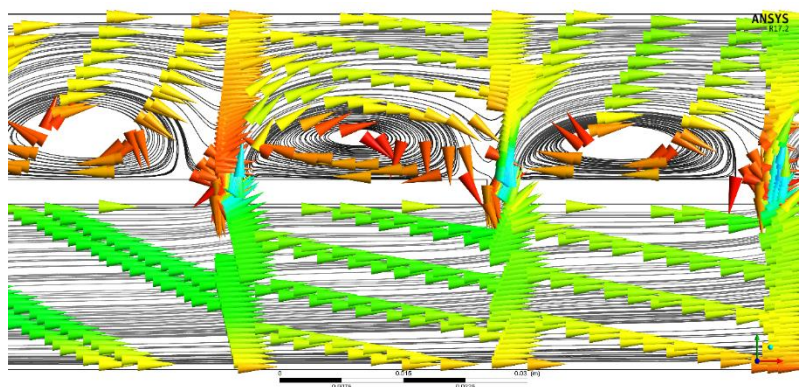

(b)

Fig. 5. Velocity vector for Case1 a) Computational domain, b) Exaggerated view.

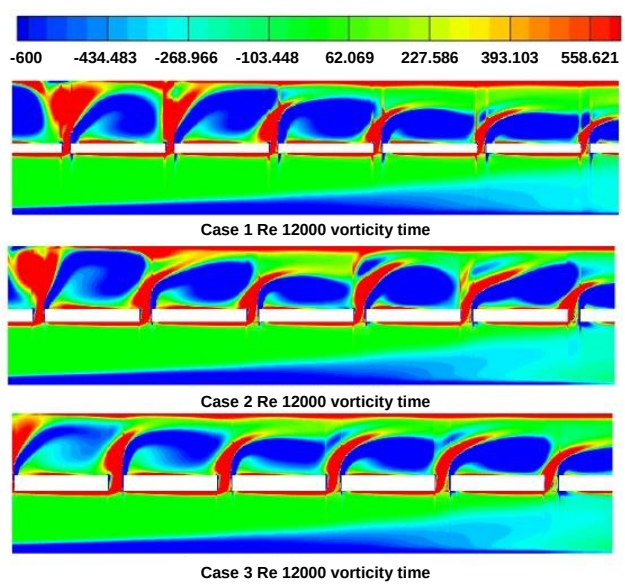

Fig. 6. Average vorticity projection along the mid-x-y axis for Re = 12000 for Case 1, Case2 and Case 3.

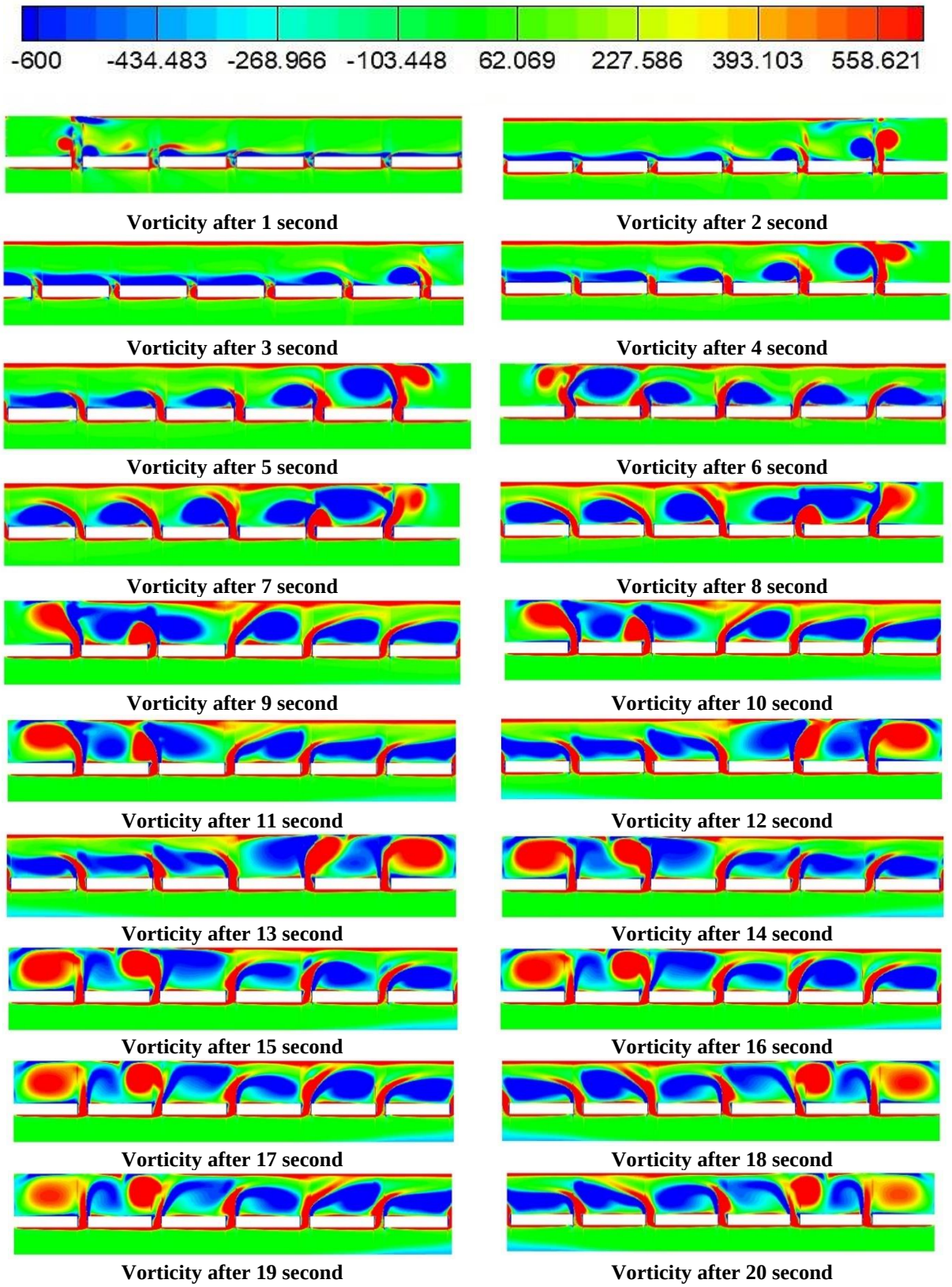

Fig. 7. Instantaneous vorticity in the jet impingement domain at various time intervals.

To better understand the vorticity and flow physics, transient results of vorticity are represented in Fig. 7. The space between each jet and the plate created a complex flow environment, characterized by peripheral vortex formations around each jet and an upwash fountain flow at the point of jet impact represented in Fig. 7. The size and positioning of these peripheral vortices, relative to the plate spacing, were determined by the nozzle design. Each case corresponded to a unique jet diameter. The decrease in impact velocity (Fig. 8) with an increasing jet diameter on the target surface resulted in lower heat transfer efficiency. As shown in Fig. 7, the vorticity profile for the 2D simulation exhibited varying time intervals, reflecting an increase in turbulence as time progressed. The localized, swirling motion of particles within a fluid flow is termed "vorticity." Fluid motion, prompted by buoyancy effects or other dynamic factors, can give rise to vorticity within a heat transfer scenario. The convective heat transfer rate within a fluid can be influenced by its vorticity and the formation of prevailing flow patterns. Fig. 7 clearly illustrates that the distribution and transmission of heat in transient heat transfer can be impacted by fluctuations in vorticity as the flow progresses. Fig. 9 shows the Average Temperature contour at Re 12000 for different cases for a certain duration.

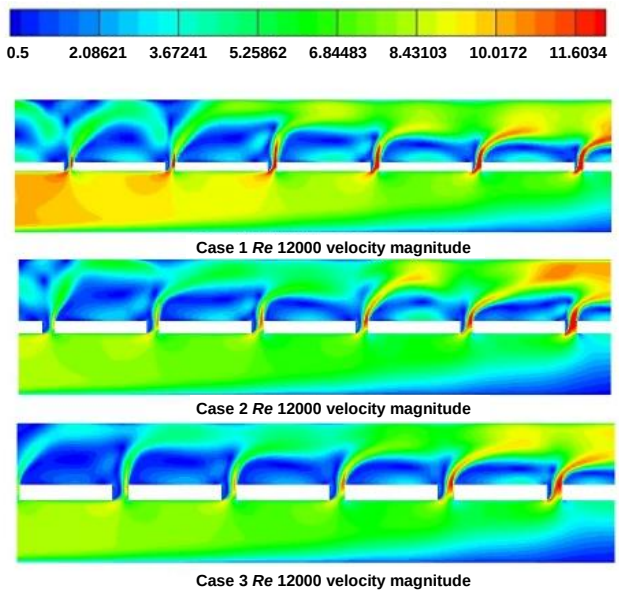

Fig. 8. Average flow velocity magnitude projection along the mid-x-y axis for Re = 12000 for Case 1, Case 2 and Case 3.

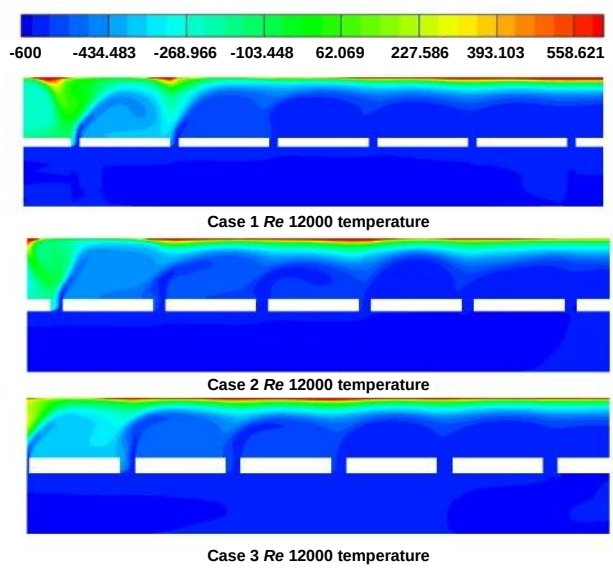

Fig. 9. Average temperature contour at Re = 12000 for Case 1, Case 2 and Case 3.

As the diameter of the jet increases hot zone created which decreases the heat transfer rate and these results are consistent with the results presented in Fig. 4 to 8.

3.2 Effects of Re and H/D ratio on local and average heat transfer and friction factor

Fig. 10 illustrates a peak maximum Nu value ranging between 80 and 90, corresponding to a jet with a diameter of 4 mm i.e. Case 2 and an X/L ratio of 0.22. Initially, Nu increases as X/L values rise, reaching its maximum at instance 2 when the jet diameter is 4 mm and the equivalent X/L value is approximately 0.2. Beyond this point, Nu starts to decline. The characteristics of the fluid, its velocity, temperature gradients, and the shape of the surface all contribute to the local Nu value. This value can vary across the surface of an object or within a fluid flow, indicating changes in flow patterns, boundary conditions, and other factors. The results validated with the contours and streamlines presented in Fig. 4 to 8.

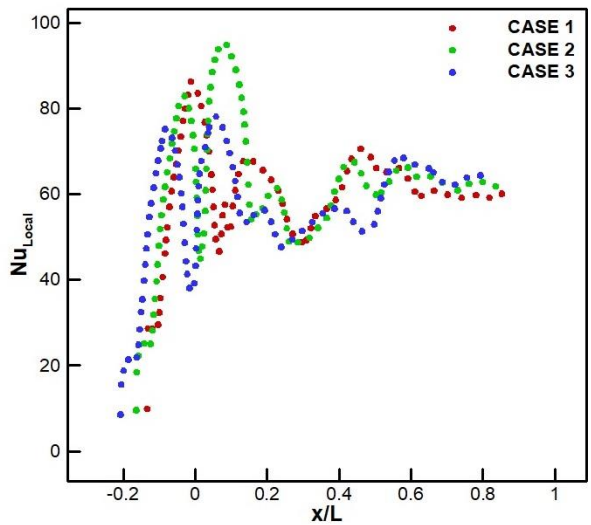

Fig. 10. Local Nusselt number Nu local variation along the jet plate length for Case 1, Case 2, and Case 3.

The results of average Nu presented in Fig. 11 and this is clearly observed that the maximum Nu is obtained for Case 1 at lower Re and with increase of Re the Nu for Case 2 is dominant.

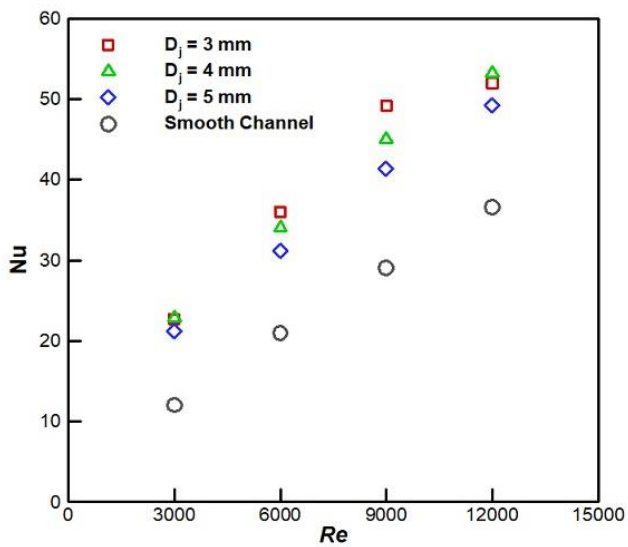

Fig. 11. Variation of Nu with Re for different jet diameters.

Fig. 12 clearly illustrates that the f decreases as Re increases. At a Re of approximately 12,000, the largest f observed for a jet with a diameter of 3 mm.

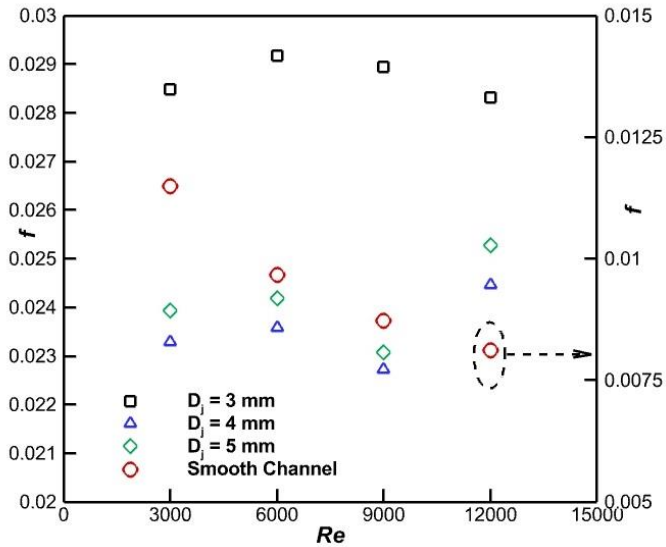

Fig. 12. Variation of f with Re for different jet diameters.

The effect of using jet impingement on smooth channel in terms of Nu and f is represented in Fig. 13 for 2 D model and smooth channel in Fig. 14 represents the relation of Nu/Nu_s with Re at different jet diameter, respectively. The value of Nu for jet impingement in all cases is more than smooth channel thus contributing to Nu/Nus causes greater than unity. The maximum enhancement is obtained at lower Re and jet diameter of 4mm. However, the increase in heat transfer increases friction penalty and significant increase in the friction factor for jet impingement is reported in Fig. 14 over smooth channel. The maximum enhancement in friction factor is attained at maximum Re and jet diameter of 3mm. To mark a tradeoff between heat transfer and friction factor thermohydraulic performance parameters defined as TEF is used to have compromise between Nu and f for jet impingement. The value of TEF greater than unity clearly signifies the dominance of jet impingement system over smooth channel and in the present case for most of the studied cases the TEF value is greater than unity as depicted in Fig. 15. The maximum TEF of 1.5 is obtained for Re = 3000 and Dj = 4 mm. as the Reynolds number increases the TEF values decreases at Re=3000 and Dj=4 mm the TEF is maximum.

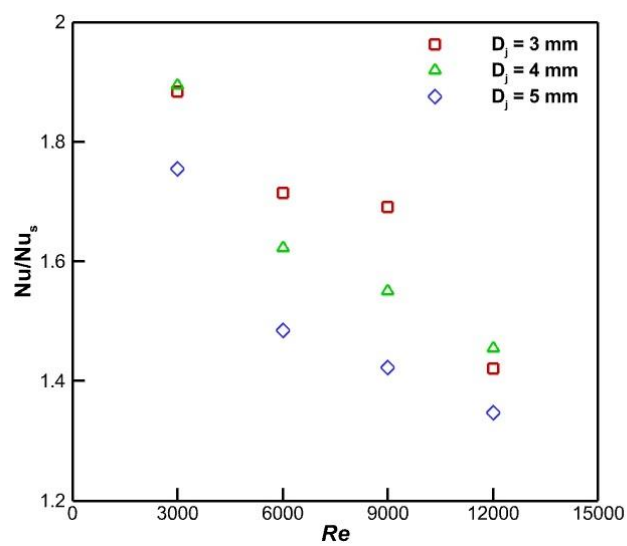

Fig. 13. Variation of Nu/Nus with Re for different jet diameters.

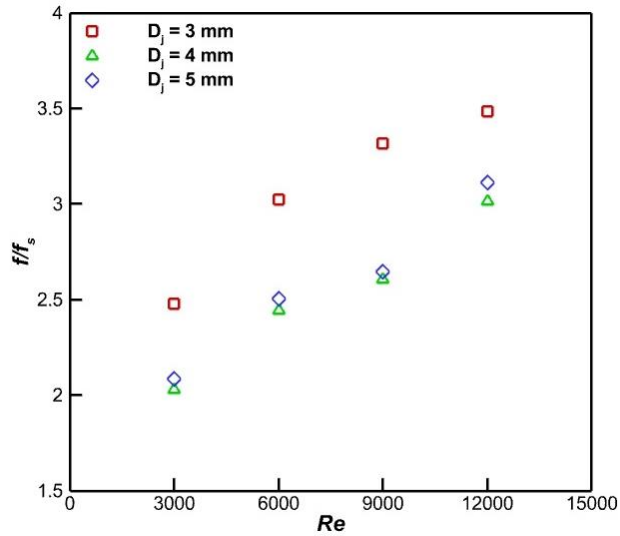

Fig. 14. Variation of f/fs with Re at different jet diameters.

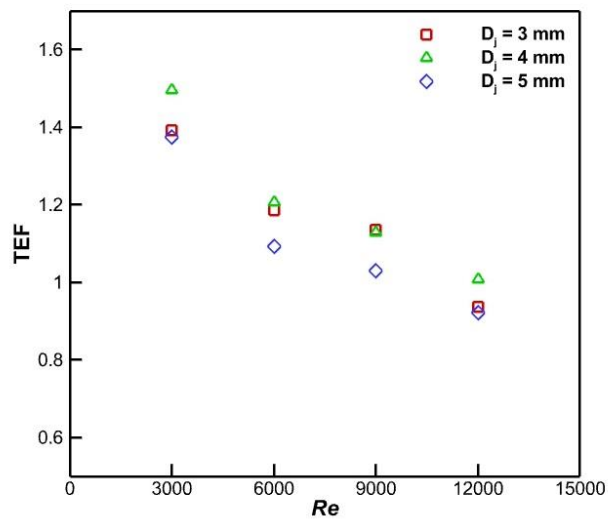

Fig. 15. Variation of TEF with Re for different jet diameters.

4. Conclusion

• Jet-to-Plate Distance Impact on Heat Transfer:
- Heat transfer near the stagnation point intensifies with decreasing jet-to-plate distance.
- Conversely, heat transfer near the boundary point decreases under the same conditions.
- Transient heat transfer consistently increases with higher Reynolds numbers for all cases.

• Reynolds Number and Flow Structure:
- Increasing Reynolds number primarily affects the velocity magnitude of the flow.
- Flow field distribution changes are contingent on the ratio of H/D.
- A lower H/D shifts the vortex center from the boundary to the stagnation point, detrimentally affecting boundary point heat transfer.

• Temperature Differences and Cooling Times:
- Temperature differences during quenching initially rise, then decline across all cases.
- The cooling time at which temperature difference peaks decreases with higher Reynolds numbers.
- Larger H/D ratios result in a smaller temperature gradient across the entire surface, promoting heat transfer uniformity.

Nomenclature

D_j	Diameter of jet
f/fs	Friction factor Ratio with smooth duct
H/D	Jet height to Hydraulic diameter ratio
D	Hydraulic diameter
TEF	Thermo-hydraulic performance
H	Height of air jet to target surface
SAH	Solar air heater
Re	Reynolds Number
SAHJI	Solar air heater jet impingement
Nu	Nusselt Number
X/D	Streamwise pitch ratio
Nu/Nus	Ratio of Nusselt Number with smooth duct
f	Friction factor
Dj/D	Spanwise pitch Ratio

References

[1] Bisht YS, Pandey SD, Chamoli S. Jet impingement technique for heat transfer enhancement: discovering future research trends. Energy Sources A: Recovery Util Environ Eff. 2023;45(3):8183-8202.

[2] Sheikholeslami M, Ali Farshad S, Ebrahimpour Z, Said Z. Recent progress on flat plate solar collectors and photovoltaic systems in the presence of nanofluid: a review. J Clean Prod. 2021;293:126119.

[3] Pukhovoy MV, Bykovskaya EA, Kabov OA. Extreme heat fluxes and heat transfer mechanisms during electronics spray and jet impingement cooling with boiling. J Phys Conf Ser. 2020;1677:012150.

[4] Diop SN, Dieng B, Senaha I. A study on heat transfer characteristics by impinging jet with several velocities distribution. Case Stud Therm Eng. 2021;26:101111.

[5] Jiang Y, Hajivand M, Sadeghi H, Barzegar Gerdroodbary M, Li Z. Influence of trapezoidal lobe strut on fuel mixing and combustion in supersonic combustion chamber. Aerosp Sci Technol. 2021;116:106841.

[6] Farnham C, Emura K, Mizuno T. Evaluation of cooling effects: outdoor water mist fan. Build Res Inf. 2015;43(3):334-345.

[7] Bisht YS, Pandey SD, Chamoli S. Experimental investigation on jet impingement heat transfer analysis in a channel flow embedded with V-shaped patterned surface. Energy Sources A: Recovery Util Environ Eff. 2023;45(4):12520-12534.

[8] Jiang Y, Abu-Hamdeh NH, Batan RAR, Li Z. Influence of upstream angled ramp on fuel mixing of hydrogen jet at supersonic cross flow. Aerosp Sci Technol. 2021;119:107099.

[9] Sheikholeslami M, Farshad SA. Numerical simulation of effect of non-uniform solar irradiation on nanofluid turbulent flow. Int Commun Heat Mass Transf. 2021;129:105648.

[10] Yaga M, Wakuta T, Reji RV, Kim HD. Effect of coaxial airstream on high-pressure submerged water jet. In: Suryan A, Doh D, Yaga M, Zhang G, editors. Recent Asian Research on Thermal and Fluid Sciences. Lecture Notes in Mechanical Engineering. Singapore: Springer; 2020. p. 1-9.

[11] Jiang Y, Moradi R, Abusorrah AM, Hajizadeh MR, Li Z. Effect of downstream sinusoidal wall on mixing performance of hydrogen multi-jets at supersonic flow: numerical study. Aerosp Sci Technol. 2021;109:106410.

[12] Nuntadusit C, Wae-hayee M, Kaewchoothong N. Heat transfer enhancement on asurface of impinging jet by increasing entrainment using air-augmented duct. Int J Heat Mass Transf. 2018;127:751-767.

[13] Said Z, Syam Sundar L, Tiwari AK, Ali HM, Sheikhleslami M, Bellos E, et al. Recent advances on the fundamental physical phenomena behind stability, dynamic motion, thermophysical properties, heat transport, applications, and challenges of nanofluids. Phys Rep. 2022;946:1-94.

[14] An Q, Dang J. Cooling effects of cold mist jet with transient heat transfer on high-speed cutting of titanium alloy. Int J Precis Eng Manuf Green Technol. 2020;7:271-282.

[15] Sheikholeslami M, Jafaryar M, Said Z, Alsabery AI, Babazadeh H, Shafee A. Modification for helical turbulator to augment heat transfer behavior of nanomaterial via numerical approach. Appl Therm Eng. 2021;182:115935.

[16] Yang M, Li C, Zhang Y, Jia D, Zhang X, Hou Y, et al. Microscale bone grinding temperature by dynamic heat flux in nanoparticle jet mist cooling with different particle sizes. Mater Manuf Process. 2018;33(1):58-68.

[17] Wae-hayee M, Yeranee K, Suksuwan W, Alimalbari A, Sae-ung S, Nuntadusit C. Heat transfer enhancement in rotary drum dryer by incorporating jet impingement to accelerate drying rate. Dry Technol. 2021;39(10):1314-1324.
[18] Khangembam C, Singh D, Handique J, Singh K. Experimental and numerical study of air-water mist jet impingement cooling on a cylinder. Int J Heat Mass Transf. 2020;150:119368.
[19] Nayak SK, Mishra PC. Thermal characteristics of air-water spray impingement cooling of hot metallic surface under controlled parameter conditions. J Therm Sci. 2016;25(3):266-272.
[20] Rajarajeswari K, Alok P, Sreekumar A. Simulation and experimental investigation of fluid flow in porous and non-porous solar air heaters. Sol Energy. 2018;171:258-270.